ISSN 1061-933X, Colloid Journal, 2021, Vol. 83, No. 5, pp. 546–557. © Pleiades Publishing, Ltd., 2021.
Russian Text © The Author(s), 2021, published in Kolloidnyi Zhurnal, 2021, Vol. 83, No. 5, pp. 512–523.

The Regularities of Coagulation in Polydisperse Zirconia Nanosol

A. V. Volkova[a], *, D. A. Vdovichenko[a], E. V. Golikova[a], and L. E. Ermakova[a]

[a] *St. Petersburg State University, St. Petersburg, 199034 Russia*

**e-mail: anna.volkova@spbu.ru*

Received April 27, 2021; revised May 5, 2021; accepted May 12, 2021

Abstract—Aggregative stability of a polydisperse zirconium oxide sol with average sizes of primary particles and aggregates equal to 24 and 95 nm, respectively, has been studied within a wide range of sodium chloride concentrations (3×10^{-3}–1 M) by turbidimetry and dynamic light scattering. The experiments have been performed at pH 4.2 and 5.6, when sol particles are positively charged, and at pH 11, when they are negatively charged. The regions of weak and intense slow coagulation, as well as the region of fast coagulation, have been determined and characterized. It has been shown that, in most cases, the thresholds of the intense slow coagulation determined from the concentration dependences of the optical density and the average particle size coincide with each other within the experiment error. Assumptions have been brought out on the coagulation mechanism and its changes upon the passages between the coagulation regions, as well as on the role of the ratios between the particle sizes of separate fractions and their amounts in the sol.

DOI: 10.1134/S1061933X21050136

INTRODUCTION

The majority of real natural and industrial disperse systems are known to be polydisperse. This circumstance is, to a considerable extent, reflected in the processes of coagulation and heterocoagulation of sols and suspensions. According to the classical ideas, the limiting case of colloidal solution instability upon its perikinetic coagulation is the process of fast coagulation, when each collision results in strong bonding of particles, while the process rate is governed only by their Brownian motion [1–3]. After the threshold of fast coagulation is reached, i.e., at an electrolyte concentration corresponding to the absence of the energy barrier that prevents particles from aggregation, a further increase in the electrolyte concentration has no effect on the particle coagulation rate [1–3] (provided that the matter does not concern ions that are specifically adsorbed under the conditions of superequivalent adsorption leading to the sign reversal of the Stern plane potential and the electrokinetic potential). Smoluchowski performed the theoretical analysis of the fast coagulation [1, 2]. According to his ideas, when colloidal particles approach each other to some distance R (radius of interparticle interaction), they irreversibly aggregate; i.e., the notion of an infinitely deep potential minimum with a vertical wall was introduced instead of the consideration of the van der Waals forces.

Several years after the formulation of the theory of fast coagulation of monodisperse systems, Müller undertook an attempt to consider the fast coagulation of polydisperse systems. He took into account the fact that Smoluchowski's assumption of the equally probable collisions between particles of the same and different sizes was not quite justified [4, 5]. According to Müller, the probability of the collision between two particles with different sizes and, especially, with shapes greatly different from the spherical one is markedly higher than that for particles with the same size. This theoretical notion was confirmed, in particular, by experiments performed by Wiegner and Marshall on studying the coagulation of sols of vanadium pentoxide and benzopurpurin [6], in which the rate of fast coagulation was 50 times higher than that calculated according to Smoluchowski. The combined analysis of the Smoluchowski and Müller theories has shown that coagulation rate ν in a two-component disperse system containing initial particles of different sizes (with radii r_{01} and r_{02}) must be higher than that calculated by the Smoluchowski theory (ν_{Sm}) for a monodisperse sol.

The coagulation of polydisperse systems was studied theoretically and experimentally in works by Friedlander [7–9], Reggy and Melik [10], and Lee [11, 12], where it was also found that the coagulation rate in polydisperse systems is higher than that in monodisperse ones. Lee [11, 12] showed that time variations in the particle size distribution upon coagulation may be described by a nonlinear integro-differential equation, which has no exact analytical solution. This equation was analytically solved either under simplified assumptions of coagulation nuclei or in an asymptotic form. Lee described the size distributions of particles of a certain volume and time variations in the

total particle number of a polydisperse sol on the basis of the condition that the initial particle size distribution in a sol may be represented by a lognormal function [11].

The authors of the aforementioned theoretical works assumed the irreversible character of the coagulation; i.e., the consideration was based on the model of the diffusion-limited cluster aggregation. In a polydisperse system, this coagulation mechanism can take place at rather high electrolyte concentrations. At lower concentrations, there is a high probability that, for relatively large particles, another model, i.e., the reaction-limited cluster aggregation, will be realized. These two models correspond to different interparticle potentials, i.e., a deep primary energy minimum in the absence of a barrier in the first case and the existence of an energy barrier before such minimum in the second case. This may, in turn, lead to the appearance of several coagulation thresholds. Moreover, in real polydisperse systems, the coagulation of an ensemble of particles may be complicated by the fact that particles may form relatively weak (in some cases, easily disintegrating) aggregates in the secondary or limited primary minima in the dependences of interparticle pair interaction energy on the interparticle distance.

The study and development of mathematical methods for the solution of kinetic equations describing the evolution of the function of particle distribution over masses at a preset probability of their collision and aggregation are among the problems of the macrokinetic theory of coagulation. At present, many theoretical works are available devoted to the aggregation kinetics of particles, with works [10, 13–22] deserving special attention.

Experimental studies of the coagulation kinetics of colloidal systems with relatively low polydispersity have shown that the coagulation has, as a rule, a stepwise character. As electrolyte concentration and observation time increase, the sol polydispersity markedly grows [23–26]. However, it should be noted that, in the literature, there are few works devoted to detailed studying the stability of polydisperse systems, in which the found threshold electrolyte concentrations (i.e., the boundaries of different regions of coagulation) are interpreted taking into account the discrete character of the particle size spectrum. In this connection, it is obvious that there is a need to develop the ideas of coagulation in real polydisperse systems, in particular, in sols obtained from air-dried nanopowders. This is all the more important, because the fields of the practical application of nanodispersions are being actively developed.

Zirconium oxide is a material on which an increasing attention is focused owing to its unique mechanical properties. ZrO_2 may be used as an adsorbent, a catalyst, and an ion exchanger. A great interest in nanoceramics based on ZrO_2 is due to its high service characteristics, such as mechanical strength, chemical and thermal stability, antibacterial activity, biocompatibility, etc. [27–31].

The goal of this work was to study in detail the stability and coagulation of ZrO_2 sols in NaCl solutions at different pH values by turbidimetry and dynamic light scattering with the aim of determining the effect of the polydispersity of an initial sol on the features of its coagulation.

EXPERIMENTAL

Zirconia hydrosol, stable to aggregation and sedimentation in initial state and prepared from commercial ZrO_2 nanopowder (Vecton, Russia), was chosen as an object of the study. Its BET specific surface area S_{sp} determined by measuring nitrogen thermal desorption with chromatographic registration was 44 m^2/g. Average size d_0 of primary nanoparticles calculated by equation

$$d_0 = 6/\rho S_{sp}, \quad (1)$$

where $\rho = 5.68$ g/m^3 is zirconium oxide density, was 24 nm.

Initial ZrO_2 powder was purified three times by electrodialysis, while drying the oxide between the dialysis cycles (after water was completely evaporated at a temperature of no higher than 80°C, zirconium oxide was dried for 1 h initially at 120 and, then, at 200°C). The efficiency of this process was judged by changes in the isoelectric point (IEP) of zirconium oxide. The successive purification of commercial ZrO_2 powder shifted its IEP in a 10^{-2} M sodium chloride solution (Fig. 1) from pH 6.5 for the powder purified one time to pH 6.1 for the twice purified oxide. The third cycle of electrodialysis caused no noticeable changes in both the electrokinetic potential and the position of the IEP, thereby suggesting the complete purification of the oxide surface. Thus, the IEP of the studied ZrO_2 powder was at pH 6.1. This value was within the range of the magnitudes reported in the literature for this oxide [32]. The triply purified powder was used for subsequent studying the stability and coagulation of zirconium oxide sols.

Zirconium oxide hydrosol stable with respect to aggregation and sedimentation was prepared from its aqueous suspension with a concentration of 0.01 wt %. For this purpose, purified oxide powder was dispersed in water for 3 h in a RELTEK USB-7/100-TNM ultrasonic bath operating at a frequency of 60 kHz. Then, the obtained 0.01% dispersion was left for a long time (nearly 2 weeks), after that the upper fraction (most finely dispersed) was taken and diluted with deionized water. The optical density of the sol thus obtained was 0.378 ± 0.005.

The effects of pH (at its initial value equal to 5.6 in the absence of additives of acid or alkali solutions and at pH 4.2 and 11) and the concentration of NaCl

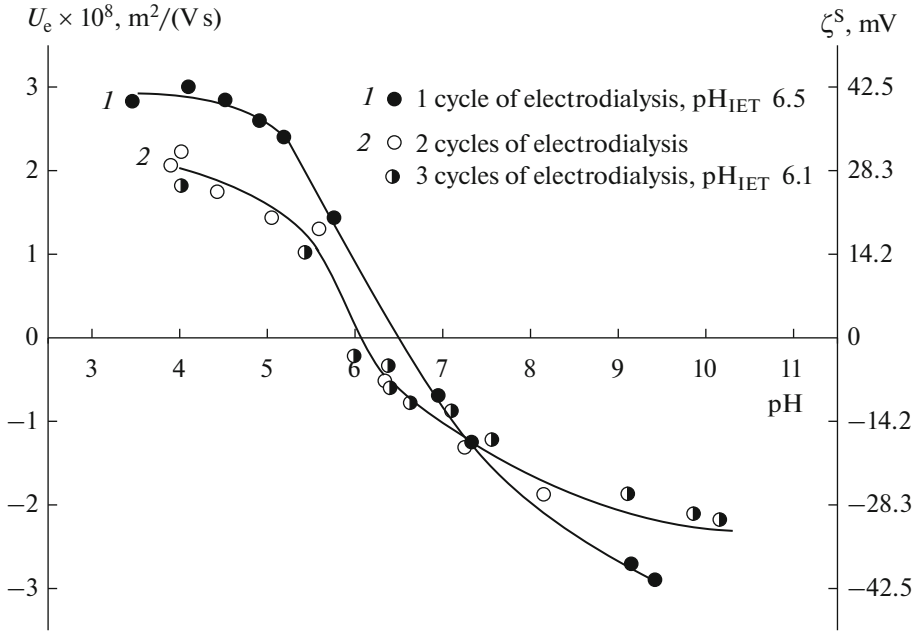

Fig. 1. The pH dependences for electrophoretic mobility U_e and electrokinetic potential ζ^S of zirconium oxide particles purified by electrodialysis in a 10^{-2} M NaCl solution.

(3×10^{-3}–1 M) as a background electrolyte on the aggregative stability of the diluted ZrO_2 hydrosol were studied in this work. The aggregative stability of the hydrosol was studied by turbidimetry, which is based on measuring the time dependence of system optical density D, and dynamic light scattering (DLS).

The turbidimetric measurements were performed in a cell 5 cm long and 2 cm wide using a KFK -3-01 photoelectrocolorimeter operating at a wavelength of 380 nm, which corresponded to the absorption maximum. Deionized water was used as a reference. To obtain dispersions with a necessary concentration of the coagulant, equal volumes of the prepared stable sol and an electrolyte solution with a doubled concentration or (in the absence of the electrolyte) deionized water were mixed using a piston mixer. Mixing was performed in counterflows in a T-shaped channel, from which the mixture was passed immediately into the measuring cell. The moment of mixing the sol and electrolyte was taken as a reference point. The measurements were carried out for 15 min. The obtained data were used to plot the dependences of optical density D on time t. The pH value of the medium was varied by adding different volumes of 0.1 M solutions of HCl or NaOH to water or a background electrolyte solution before they were added to a zirconium oxide dispersion. At the zero salt concentration, the values of the optical density remained unchanged during the entire experiment time at all pH values.

After the measurements of the optical density at a fixed electrolyte concentration were completed (nearly 20 min after mixing the sol with the sodium chloride solution), the sizes and electrokinetic potentials of ZrO_2 particles were determined. The particle size distributions (PSDs) and the average particle sizes in the studied sols and electrophoretic mobilities U_e of the particles were determined at different pH values and electrolyte concentrations using a Zetasizer Nano ZS analyzer (Malvern Instruments, United Kingdom) by DLS (detection angle of 173°) and laser Doppler electrophoresis, respectively. The sol samples were preliminarily thermostated for 2 min at 20°C in a DTS1070 universal U-shaped cell equipped with integrated gold-plated electrodes. The error in the measurement of the U_e values was $\pm(0.1–0.2)$ m^2/(V s). Electrokinetic potential ζ^S was calculated by the Smoluchowski equation

$$\zeta^S = \frac{\eta}{\varepsilon\varepsilon_0} U_e, \quad (2)$$

where η is the dynamic viscosity of a medium and ε and ε_0 are the dielectric permittivities of the medium and vacuum, respectively.

In addition, the values of the electrophoretic mobility experimentally found for the lowest values of electrokinetic radius ka (where k is the Debye parameter and a is the primary particle radius equal to 12 nm) with allowance for the polarization of electrical double layer were used to calculate the values of electrokinetic potential ζ^W within the framework of the Overbeek–Boes–Wiersema model [33].

The optical density of the studied zirconium oxide hydrosol obtained by two-fold dilution of a sol with an optical density of 0.378 ± 0.005 was 0.189 ± 0.005. The

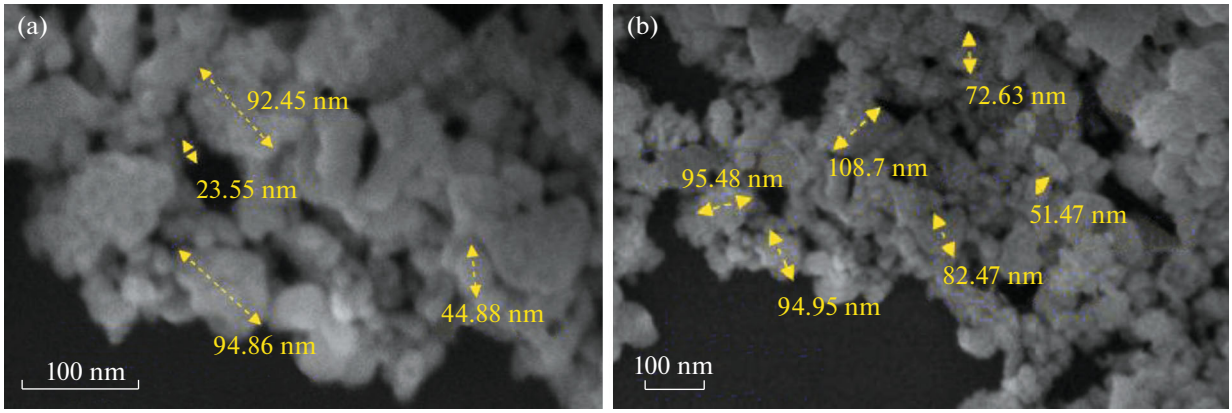

Fig. 2. Electron micrographs of zirconium oxide hydrosol particles.

size and morphology of ZrO_2 sol particles were also determined by scanning electron microscopy (SEM) with a Zeiss Merlin instrument. The micrographs presented in Fig. 2 show that the sol was polydisperse and contained both individual (primary) particles, whose most probable size was close to $d_0 = 24$ nm, and their (primary) aggregates having an almost spherical shape and a prevailing size of 40–120 nm.

The results obtained by DLS agree with the SEM data. The initial ZrO_2 sol, which is stable with respect to sedimentation and aggregation, had a rather narrow PSD (Fig. 3); its polydispersity index was PdI = 0.13, average size of primary aggregates d_{0I}^{agg} determined from the intensity distribution over sizes was 95 nm, and the range of particle sizes was 32–220 nm. However, it should be noted that, in our case, DLS does not provide information on particles smaller than 30 nm, i.e., on the primary particles, which, according to SEM data, are present in the sol in a rather large amount (Fig. 2). Moreover, it is worth noting that the PSDs determined at the studied pH values are close to each other.

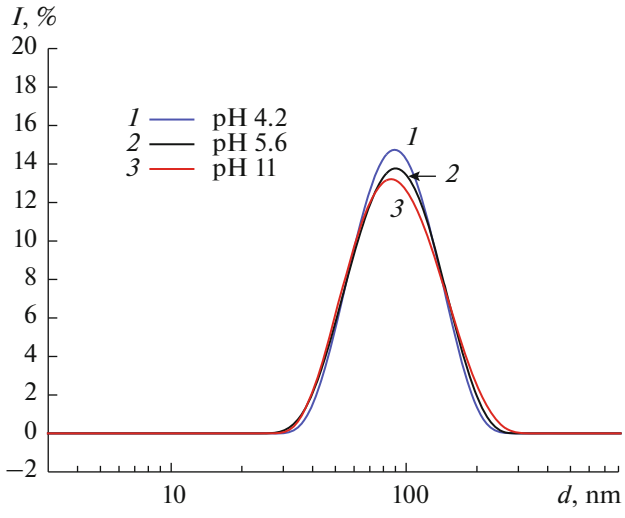

Fig. 3. Dependences of scattered light intensity on particle size in initial ZrO_2 sol stable with respect to sedimentation and aggregation at pH values of (*1*) 4.2, (*2*) 5.6, and (*3*) 11.

Laser flow ultramicroscopy [34] was employed to determine the number concentration of sol particles detectable by this method, i.e., relatively large aggregates. This concentration appeared to be 1.2×10^8 cm^{-3}.

The solutions and dispersions were prepared using deionized water with an electric conductivity of no higher than 1.5×10^{-6} Ω^{-1} cm^{-1} (Aqualab AL Plus water-purification system). The pH values of the media were measured with a SevenMulti pH meter (Mettler Toledo).

RESULTS AND DISCUSSION

Figure 4 shows the turbidimetry data on the aggregative stability of ZrO_2 sol in NaCl solutions at pH 5.6, when the sol particles are positively charged. The analysis of the time dependences of the sol optical density at its natural pH has shown that the pattern of the $D(t)$ curves in an electrolyte concentration range of 3×10^{-3} M $< C_{NaCl} \le 2 \times 10^{-2}$ M is typical for the slow coagulation (SC), while, at $C_{NaCl} > 2 \times 10^{-2}$ M, it is characteristic of the fast coagulation (FC).

It has been shown [24] that, for polydisperse sols of oxides, the intensity of the SC process may be different depending electrolyte concentration, thereby causing the appearance of the regions of weak and intense SC. Taking into account this fact, the exact values of the coagulation thresholds were determined by plotting the dependences of hydrosol optical density on salt solution concentration at a fixed observation time (Fig. 5). The threshold of fast coagulation (C_{FC}) was determined at a short observation time ($t = 0.5$ min; Fig. 5, curve *1*) by extrapolating the linear region of the D–log$C$ dependence, with the maximum values of dD/dC being inherent in this region, to the line corre-

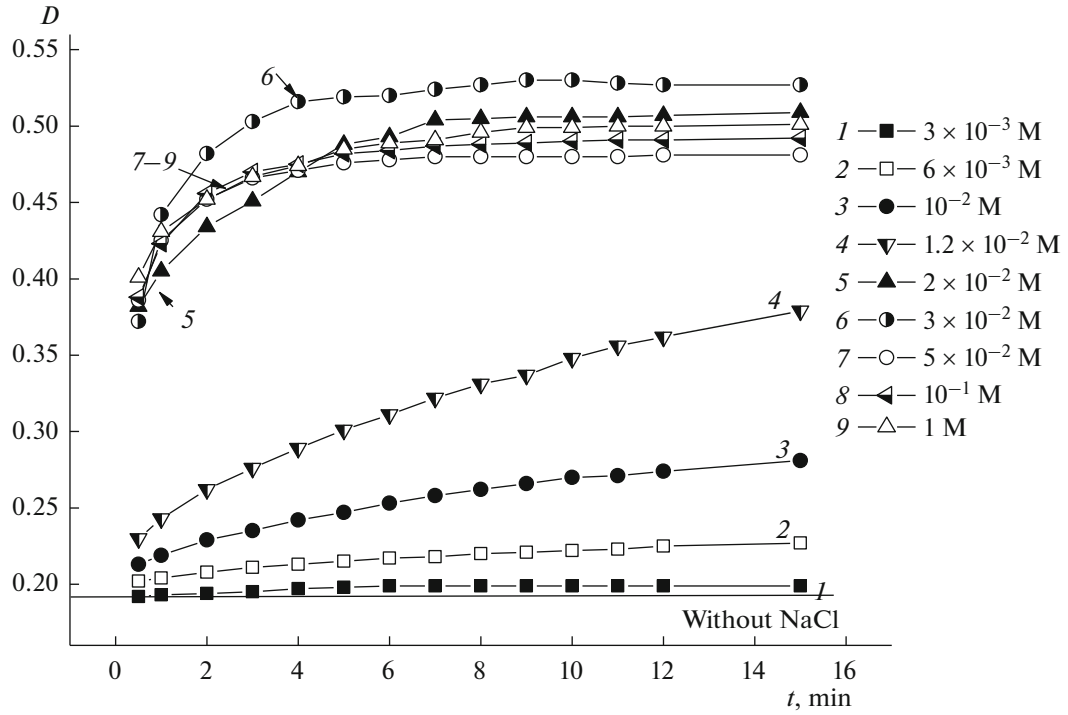

Fig. 4. Dependences of the optical density of ZrO_2 hydrosol containing positively charged particles on observation time at natural pH 5.6 and different NaCl concentrations.

sponding to constant values of the optical density at high concentrations of the background electrolyte. At the maximum observation time (t = 15 min; Fig. 5, curve *2*), the extrapolation of the linear region of the D–log$C$ dependence to the line of sol stability yielded the exact value of the threshold of intense SC (C_{ISC}).

The thresholds of the intense slow and fast coagulation processes determined graphically at pH 5.6 have appeared to be 8.5×10^{-3} and 2.3×10^{-2} M, respectively (Fig. 5, Table 1). For the threshold of the weak SC (C_{WSC}), we, using the available experimental data, have managed to determine reliably only a range of possible electrolyte concentrations: 3×10^{-3} M < $C_{WSC} \le 6 \times 10^{-3}$ M. It should be noted that, at the natural pH value, the threshold NaCl concentrations are rather low. The thresholds of ZrO_2 sol coagulation at pH 4.2 and 11 were determined analogously, and the results are presented in Table 1.

By analyzing the time dependences of ZrO_2 sol optical density at pH 4.2, when the sol particles were also charged positively, it was shown (Fig. 6) that the system was stable at $C_{NaCl} \le 3 \times 10^{-2}$ M, while SC and FC occur at concentrations of 3×10^{-2} M < $C_{NaCl} \le 1 \times 10^{-1}$ M and $>10^{-1}$ M, respectively. The threshold of intense SC (C_{ISC}) determined graphically was 6.8×10^{-2} M (Table 1).

We failed to determine exactly the thresholds of FC and weak SC from the available experimental data: $C_{FC} > 10^{-1}$ M and 3×10^{-2} M < $C_{WSC} \le 5 \times 10^{-2}$ M. Note that, the threshold NaCl concentrations at pH 4.2 are almost an order of magnitude higher than the corresponding values at the natural value of sol pH. This seems to be related to a rise in the contribution of the repulsive ion-electrostatic forces to the total pair interparticle interaction energy because of the higher electrokinetic potential of the particles at acidic pH values. Indeed, the analysis of the data on the ζ-potential of zirconium oxide particles has indicated that, at a constant electrolyte solution concentration, the values of the electrokinetic potential at pH 4.2 are higher than those at pH 5.6 (Fig. 7).

The analysis of the time dependences for the optical density of the ZrO_2 sol at pH 11, when the sol particles are charged negatively, has shown (Fig. 8) that the system is stable at $C_{NaCl} \le 10^{-2}$ M, while, at a sodium chloride concentration of 2×10^{-2} M, SC is already observed, and, at $C_{NaCl} \ge 5 \times 10^{-2}$ M, FC takes place.

It is seen in Fig. 9 (curve *2*) that, for the sol of negatively charged particles, the region of the weak SC is either absent or observed in a very narrow concentration range of $10^{-2} < C_{WSC} < 2 \times 10^{-2}$ M. The thresholds graphically determined for intense SC and FC are 2×10^{-2} and 5.0×10^{-2} M, respectively (Fig. 9, Table 1). The threshold NaCl concentrations at pH 11 are higher than those at the natural pH (see Table 1) because of the difference in the absolute values of the

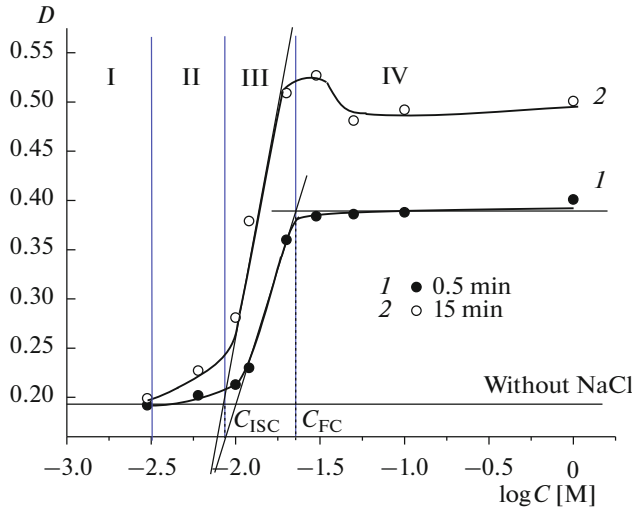

Fig. 5. Dependences of optical density of ZrO_2 hydrosol containing positively charged particles on NaCl concentration at (*1*) 0.5 and (*2*) 15 min of observation and natural pH 5.6: (I) region of stability, (II) region of weak slow coagulation, (III) region of intense slow coagulation, and (IV) region of fast coagulation.

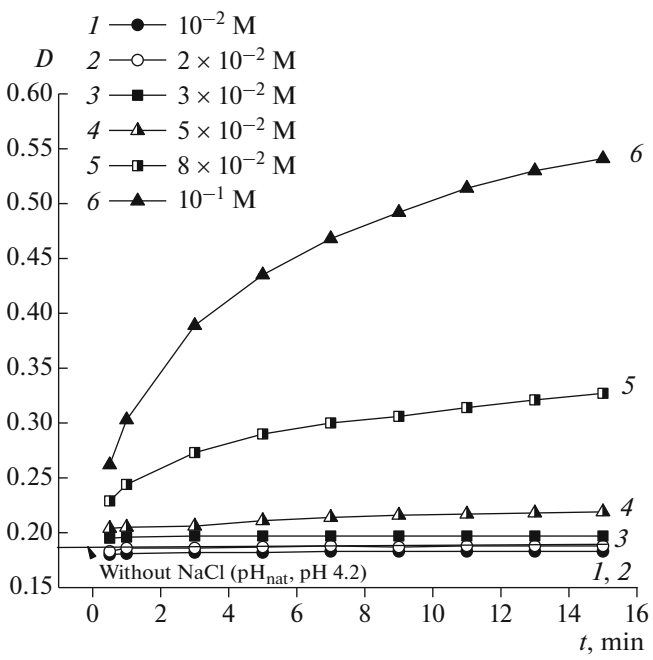

Fig. 6. Dependences of optical density of ZrO_2 hydrosol containing positively charged particles on observation time at pH 4.2 and different NaCl concentrations: (*1*) 10^{-2}, (*2*) 2×10^{-2}, (*3*) 3×10^{-2}, (*4*) 5×10^{-2}, (*5*) 8×10^{-2}, and (*6*) 10^{-1} M.

ζ-potentials of zirconium oxide particles. It should be noted that, in spite of the higher absolute values of the ζ^W-potential for particles in the alkaline pH region than those in the acidic region, the ZrO_2 sol is markedly more stable at pH 4.2 in almost the entire concentration range (Fig. 7).

The dependences of the average particle size on sodium chloride concentration determined by DLS 20 min after the addition of the electrolyte solution to the ZrO_2 sol are shown in Figs. 10–12. Note that, in some cases, two peaks arose in the PSD curves, especially in the region of intense SC. In the plots, the values corresponding to them are connected by the dashed lines, and the percentages of the corresponding parameter are presented for particles of a given size.

It follows from Figs. 10–12 that, as NaCl concentration increases and the aggregative stability of the sol is deteriorated, the average size of ZrO_2 particles increases. Moreover, at pH 5.6 and 11 it increases to close values of *d*, which are, on average, 10–20 times larger than the size of the primary aggregates in the initial sol.

Table 1. Experimental data on coagulation thresholds of ZrO_2 sols at different pH values of dispersion media

pH	Sign of particle charge	C_{WSC} and C_{ISC} (M) from *D*–log*C* curves	C_{ISC}, M			C_{FC}, M
			from d_I–log*C* curves	from d_V– log*C* curves	from d_N–log*C* curves	from *D*–log*C* curves
4.2	+	$3 \times 10^{-2} < C_{WSC} \le 5 \times 10^{-2}$, $C_{ISC} = 6.8 \times 10^{-2}$	6.9×10^{-2}	6.9×10^{-2}	8.1×10^{-2}	$>10^{-1}$
5.6	+	$3 \times 10^{-3} < C_{WSC} \le 6 \times 10^{-3}$, $C_{ISC} = 8.5 \times 10^{-3}$	9.3×10^{-3}	9.5×10^{-3}	9.7×10^{-3}	2.3×10^{-2}
11	–	$C_{ISC} = 2 \times 10^{-2}$	2.0×10^{-2}	2.2×10^{-2}	2.7×10^{-2}	5.0×10^{-2}

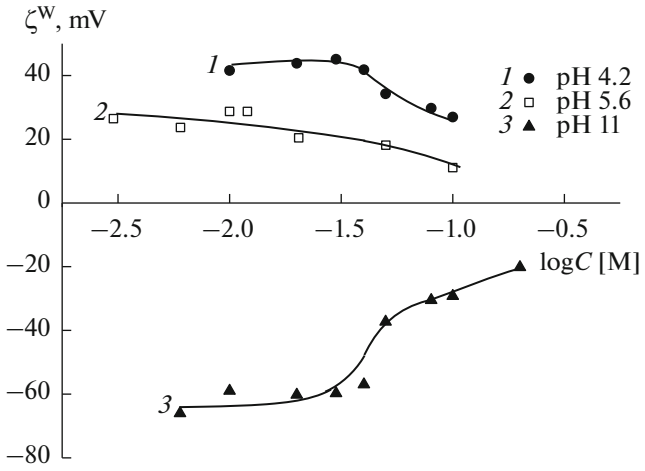

Fig. 7. Dependences of electrokinetic potential ζ^W of zirconium oxide particles on concentration of NaCl solutions at different pH values: (*1*) 4.2, (*2*) 5.6, and (*3*) 11.

The thresholds of the intense SC were also graphically determined from the curves drawn through the points corresponding to the larger average particle sizes in the case of the bimodal PSD by an extrapolation method analogous to that described above for the D–log$C$ dependence at t = 15 min. The results obtained are presented in Table 1. Note that the analysis of the concentration dependences of the average particle size at pH 11 (Figs. 10–12, curves *2*) has shown that the rate of variations in the particle size is, seemingly, almost constant throughout the region of SC. Hence, intense SC alone occurs in this region in accordance with the turbidimetry data (Fig. 9, curve *2*).

As follows from the data presented in Table 1, the values of C_{ISC} found from the concentration dependences of the optical density and the average particle size coincide within the determination error with the exception of those obtained from the d_N–log$C$ dependences at pH 4.2 and 11. In the latter case, the region of the weak SC is actually absent, and, at pH 4.2 (Fig. 12, curve *3*), the values of C_{ISC} are somewhat higher than those determined from the $D(d_I, d_V)$–log$C$ dependences, especially in the acidic pH region. This may be related to the fact that, when an acid or alkali solution is added, particle aggregates present in the initially stable hydrosol at the natural pH are partly disintegrated because of an increase in the absolute value of the ζ-potential. In addition to a decrease in the content of rather large aggregates, this leads to a rise in the number concentration of small particles (primary particles or aggregates with sizes smaller than the average size at pH 5.6) and, hence, to a decrease in the fraction of slowly coagulating small particles relative to their total amount in the dispersion. This is, most probably, the reason for the close number PSDs in the region of weak SC and in the initial part of the region of intense SC. Moreover, variations in the relations between the numbers and sizes of particles in the system may explain the appearance of the second peak with a maximum at nearly 20 nm (primary particles), which becomes "visible" in the intensity distribution

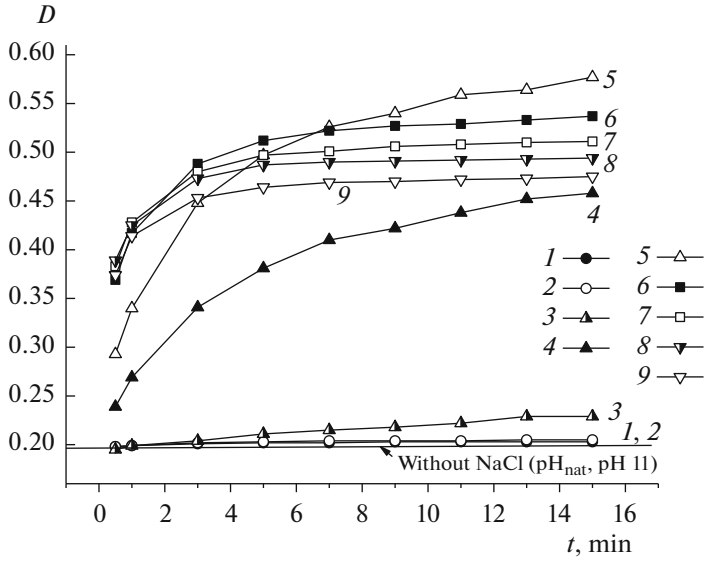

Fig. 8. Dependences of optical density of ZrO_2 hydrosol containing negatively charged particles on observation time at pH 11 and different NaCl concentrations: (*1*) 6×10^{-3}, (*2*) 10^{-2}, (*3*) 2×10^{-2}, (*4*) 3×10^{-2}, (*5*) 4×10^{-2}, (*6*) 5×10^{-2}, (*7*) 8×10^{-2}, (*8*) 10^{-1}, and (*9*) 2×10^{-1} M.

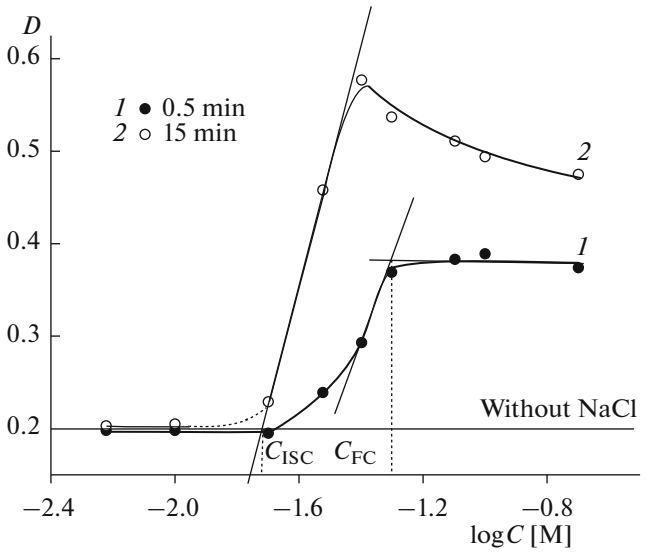

Fig. 9. Dependences of optical density of ZrO_2 hydrosol containing negatively charged particles on NaCl concentration at pH 11 and observation times of (*1*) 0.5 and (*2*) 15 min.

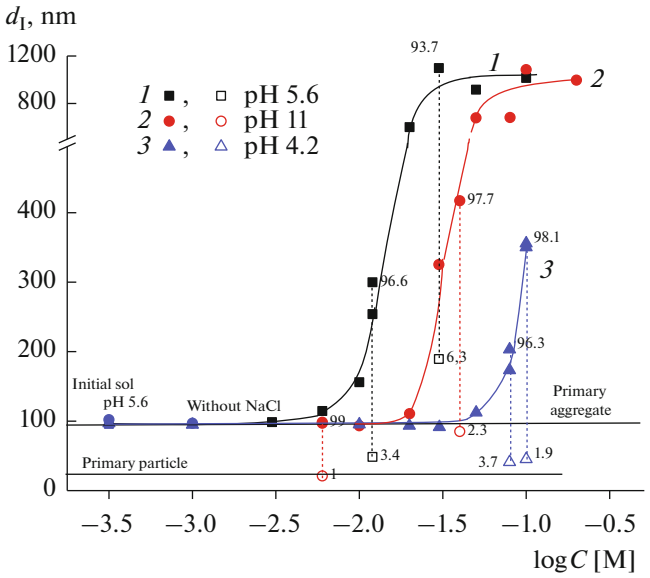

Fig. 10. Dependences of average particle diameter d_I determined for ZrO_2 hydrosol from scattered light intensity distribution over particle sizes on NaCl concentration at pH values of (*1*) 5.6, (*2*) 11, and (*3*) 4.2 and observation time of 20 min.

over particle sizes (Fig. 13a, curve *1*) for the stable hydrosol at pH 11 and NaCl concentration of 6×10^{-3} M against the background of the peak attributed to the primary aggregates. At the same time, if the contribution of "small" particles to the scattered light intensity amounts to 1% (Fig. 13a, curve *1*), their number concentration is 90.9% (Fig. 13c, curve *1*). This proves that the initial sols with monomodal PSD contain not only aggregates of primary particles, but also the particles themselves, as is seen from the SEM data (Fig. 2). The concentration of the primary particles, which are most often "invisible" for DLS, is rather high and depends on dispersion pH. Seemingly, it is this fact that explains the actual absence of the region of weak SC at pH 11, when the absolute value of the ζ-potential is maximal (Fig. 7), and, hence, the fraction of the primary particles is highest in the initial sol. Undoubtedly, the presence of "small" particles in the initial stable hydrosol makes it necessary to take into account their role when theoretically describing the stability and coagulation of polydisperse systems.

The obtained experimental data enable us to assume a possible mechanism of coagulation in a polydisperse sol containing both primary particles and aggregates thereof. To illustrate the evolution of the particle sizes of the ZrO_2 hydrosol with an increase in sodium chloride solution concentration, Fig. 13 presents the PSDs at the natural pH value.

The region of weak SC is characterized by low process rate dD/dt; a slight growth in D as compared with that of the stable dispersion even at the maximal observation time; a small increase in the PdI values (within a range of 0.01–0.02); and a slight growth in the average particle sizes, which is accompanied by a small shift of PSD toward larger sizes, with a rise in electrolyte concentration (Fig. 13, curve *3*). All these facts seem to indicate the onset of the coagulation of "small" (primary) particles or their small aggregates (corresponding to the lower limit of the PSD curve).

The region of intense SC is distinguished by a drastic (as compared with the region of weak SC) increase in the values of PdI (by 0.04–0.13), optical density and average particle size (substantial shift of PSD toward larger sizes (Fig. 13, curves *4*, *5*)); the appearance of a bimodal PSD; and an almost linear growth of D and d values corresponding to the fraction of large particles in the case of the bimodal PSD with an increase in electrolyte concentration (at t = const). All of the aforementioned may indicate the coagulation of the entire ensemble of sol particles, with the mechanism and rate of coagulation depending on salt solution concentration, particle sizes, and the contents of individual fractions in an initial dispersion. Therewith, it must be kept in mind that, even when the number concentration of large primary aggregates in a sol is very low, their coagulation may cause rather pronounced changes in the studied parameters of a system because of their strong scattering ability (much stronger than that of small particles). Moreover, it is of interest that, in a number of cases, the optical density of the sol in the region of intense SC exceeds that in the region of

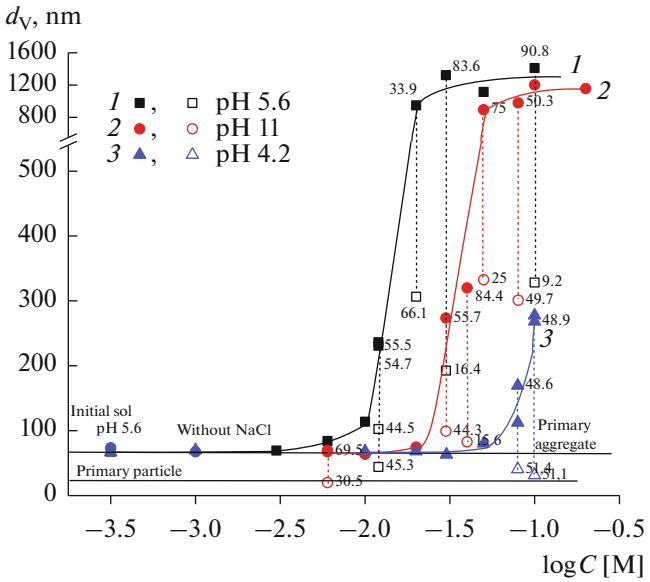

Fig. 11. Dependences of average particle size d_V determined for ZrO_2 hydrosol from particle volume size distribution on NaCl concentration at different pH values and observation time of 20 min.

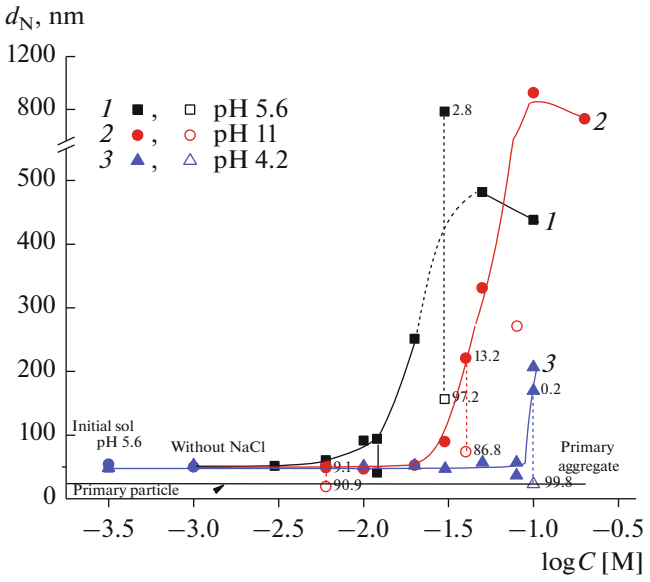

Fig. 12. Dependences of average particle size d_N determined for ZrO_2 hydrosol from particle number size distribution on NaCl at different pH values and observation time of 20 min.

FC at long observation times (Figs. 4, 8). This is possibly explained by a difference in the structures of the aggregates being formed: the fast coagulation is characterized by the formation of looser aggregates, which, therefore, have a weaker scattering ability, thereby leading to lower D values at electrolyte concentrations above the FC threshold.

It should also be noted that, in the region of intense SC, coagulation of sols with bimodal PSDs was, in some cases, accompanied by not only an increase in the average aggregate size relative to that in the stable dispersion, but also the appearance of a peak with a maximum at $d^{agg} < d_0^{agg}$ (Figs. 10–12, curves *1*, *3*) up to sizes close to the primary particle size (Fig. 12, curve *3*). Seemingly, when the rate of SC is already rather high and the average size of the particles of the large fraction increases with a simultaneous decrease in their number concentration, the relations between the sizes and amounts of scattering particles in a system drastically change, and smaller particles become also "visible." This indicates that the coagulation rate of large particles in the considered systems is, most probably, higher than that of small aggregates or primary particles; hence, the coagulation occurs via a barrierless mechanism (in the secondary potential minimum). However, it is necessary to calculate the energy of the interparticle interaction within the framework of the DLVO theory to confirm this assumption. Note that the possibility of coagulation of primary particles and aggregates with each other also cannot be excluded in the region of SC.

The region of FC at different NaCl concentrations is mainly characterized by close monomodal PSDs (Fig. 13, curves *7*, *8*), as well as close and markedly higher (in our case, by nearly 2 times) values of PdI and average particle sizes as compared with those in the stable sol. As a consequence, the optical density remains unchanged with variations in electrolyte concentration (Fig. 5, curve *2*). However, at salt solution concentrations close to threshold values C_{FC}, the region of FC may additionally be characterized by both a monomodal PSD with a maximum shifted toward smaller sizes as compared with those at $C_{NaCl} \geqslant C_{FC}$ and a bimodal PSD, with the position of the peak that characterizes the fraction of larger particles being close to the position of the peak at $C_{NaCl} \geqslant C_{FC}$ (Figs. 13a, 13b, curves *6–8*; Figs. 10, 11, curves *1*, *2*). Seemingly, this circumstance may be the reason for somewhat higher values of the optical density of the system at electrolyte concentrations close to C_{FC} than those at $C_{NaCl} \geqslant C_{FC}$, in the case of coagulation gone rather far (Fig. 5, curve *2*), while at short times t, the value of D is constant throughout the region of FC (Fig. 5, curve *1*). The analysis of the observed regularities has led us to assume that, in the initial region of FC, sol particles fast coagulate via different mechanisms, i.e., both barrier and barrierless mechanisms, depending on their sizes. Note that the assumptions brought out after the analysis of experimental data may, undoubtedly, become more justified after the

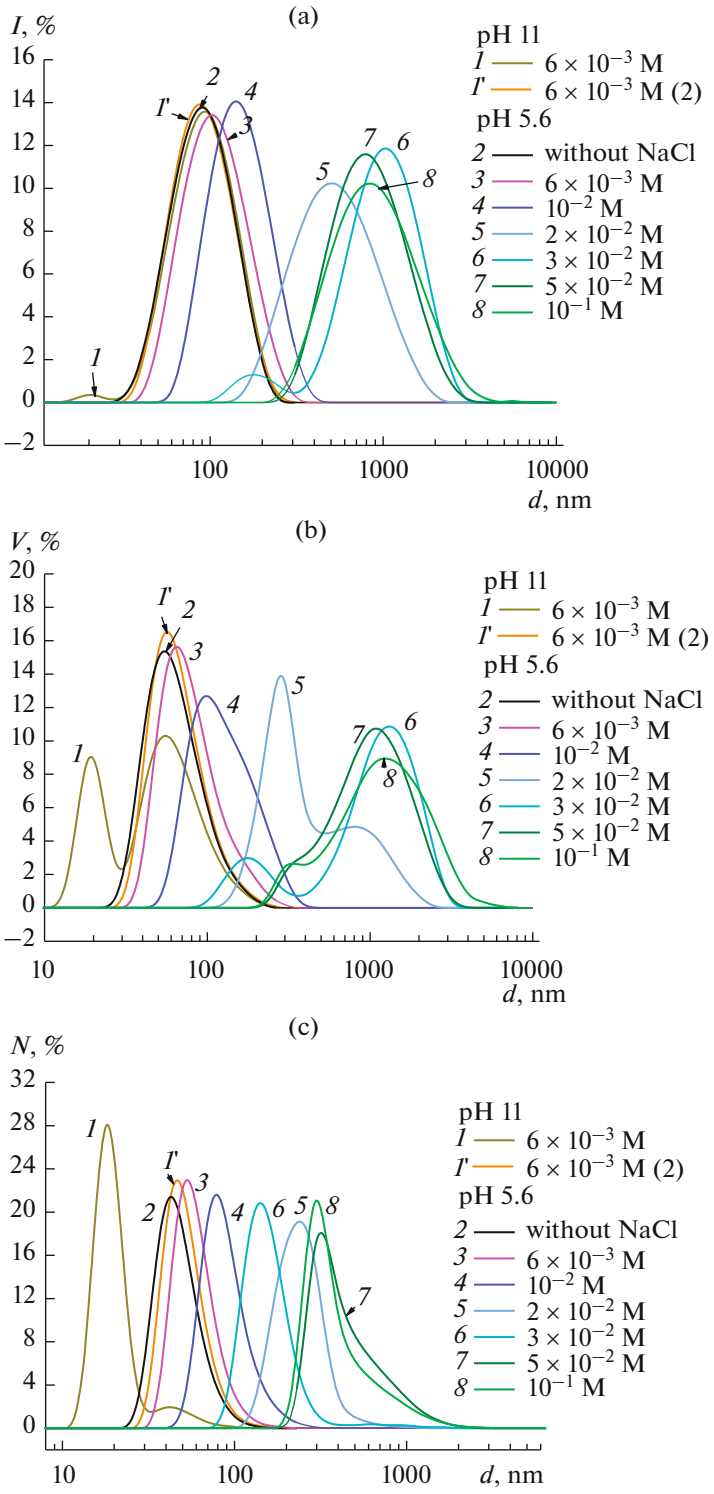

Fig. 13. Dependences of (a) scattered light intensity and (b) volume and (c) number of particles on their size in ZrO_2 sol at pH values of (*1*, *1'*) 11 and (*2*–*8*) 5.6 and different NaCl concentrations; $t = 20$ min.

comparison of the obtained results with the calculations performed within the framework of the contemporary theories of the stability of colloidal systems.

CONCLUSIONS

The aggregative stability of polydisperse zirconium dioxide sols containing both primary particles and their aggregates has been studied by turbidimetry and

dynamic light scattering in sodium chloride solutions with concentrations of 3×10^{-3}–1 M and different pH values (4.2, 5.6, 11). The thresholds of intense slow and fast coagulation have been determined graphically, and the concentration range corresponding to the onset of weak slow coagulation has been found. It has been shown that the sols are most stable at pH 4.2, in spite of the higher absolute values of the ζ^{W}-potential of particles at pH 11, while they are least stable at the natural pH 5.6, which agrees with the results of measuring the electrokinetic potential of ZrO_2 particles. In addition, it has been found that the initial ZrO_2 sol with a monomodal PSD contains both aggregates of primary particles and the primary particles themselves, with the concentration of the latter particles, which are most often "invisible" by DLS, being rather high and depending on dispersion pH.

General regularities have been revealed for the stepwise coagulation of the polydisperse ZrO_2 sol. The main specific features of each region of coagulation have been generalized, and the roles of the relations between the sizes and number concentrations of the particles of the initial polydisperse sol in a realized mechanism of coagulation and their influence on the type of the formed aggregates have been emphasized. It has been assumed that, in the region of weak SC, coagulation most probably involves "small" ZrO_2 particles, i.e., primary particles or small aggregates thereof (which correspond to the lower limit of sizes in the PSD curve for the initial sol). In the region of intense SC, which is characterized by the appearance of a bimodal PSD, the entire ensemble of particles seems to undergo coagulation.

The analysis of the experimental data has led us to assume that, both in the region of intense SC and in the initial region of FC, sol particles may coagulate via different mechanisms, i.e., the barrier and barrierless mechanisms, depending on particle sizes. In the region of intense SC, the coagulation may proceed both slowly and fast, with this circumstance being reflected in the character of PSD. In the region of FC at NaCl concentrations markedly higher than the threshold one, the entire ensemble of sol particles fast coagulates via the barrier mechanism.

ACKNOWLEDGMENTS

The study was performed using the equipment of the Interdisciplinary Resource Center for Nanotechnology of the St. Petersburg State University. The authors are grateful to D.A. Aleksandrov for the measurement of the specific surface area of zirconium oxide powder.

CONFLICT OF INTEREST

The authors declare that they have no conflicts of interest.

REFERENCES

1. Smoluchowski, M., *Z. Phys. Chem.,* 1917, vol. 92, p. 129.
2. Einshtein, A. and Smolukhovskii, M., *Brounovskoe dvizhenie* (Brownian Motion), Moscow: ONTI, 1936.
3. Kruyt, H.R., *Colloid Science,* Elsevier, 1952, vol. 1.
4. Müller, H., *Kolloid. Z.,* 1926, vol. 38, p. 1.
5. Müller, H., *Kolloid Beihefte,* 1928, vol. 26, p. 257.
6. Wiegner, G. and Marshall, C.E., *Z. Phys. Chem. A,* 1929, vol. 140, p. 39.
7. Wang, C.S. and Friedlander, S.K., *J. Colloid Interface Sci.,* 1967, vol. 24, p. 170.
8. Swift, D.L. and Friedlander, S., K, *J. Colloid Interface Sci.,* 1964, vol. 19, p. 621.
9. Friedlander, S.K., *Smoke, Dust and Haze: Fundamentals of Aerosol Behavior,* New York: Wiley, 1977.
10. Reggy, S.R., Melik, D.H., and Fogler, H.S., *J. Colloid Interface Sci.,* 1981, vol. 82, p. 116.
11. Lee, K.W., *J. Colloid Interface Sci.,* 1983, vol. 92, p. 315.
12. Lee, K.W. and Chen, H., *Aerosol Sci. Technol.,* 1984, vol. 3, p. 327.
13. Hunt, J.R., *Coagulation in Continuous Particle Size Distribution; Theory and Experimental Verification. Report No. AC-5-80,* California Institute of Technology, 1980.
14. Pen'kov, N.V., *Koagulyatsionnye protsessy v dispersnykh sistemakh* (Coagulation processes in Dispersed Systems), Yekaterinburg: Izd. Sokrat, 2006.
15. Voloshchuk, V.M. and Sedunov, Yu.S., *Protsessy koagulyatsii v dispersnykh sistemakh* (Coagulation Processes in Dispersed Systems), Leningrad: Gidrometeoizdat, 1975.
16. Elimelech, M., Gregory, J., Jia, X., and Williams, R.A., *Particle Deposition and Aggregation: Measurement, Modelling and Simulation,* London: Butterworth-Heinemann, 2013.
17. Dubovski, P.B., *Mathematical Theory of Coagulation, Lecture Notes Series,* Seoul: Seoul Natl. Univ., 1994, vol. 23.
18. Dubovski, P.B., *J. Phys. A: Math.,* 1999, vol. 32, p. 781.
19. Dubovskii, P.B., *Zh. Eksp. Teor. Fiz.,* 1999, vol. 116, p. 717.
20. Wu, K.L. and Lai, S.K., *Langmuir,* 2005, vol. 21, p. 3238.
21. Wattis, J.A.D., *Phys. D: Nonlinear Phenom.,* 2006, vol. 222, p. 1.
22. *Kinetic Aggregation and Gelation,* Family, F., and Landau, D.P., Eds., Amsterdam: Elsevier, 1984.
23. Molina-Bolıvar, J.A., Galisteo-Gonzalez, F., and Hidalgo-Alvarez, R., *J. Colloid Interface Sci.,* 1997, vol. 195, p. 289.
24. Volkova, A.V., Ermakova, L.E., and Golikova, E.V., *Colloids Surf. A,* 2017, vol. 516, p. 129.
25. Chernoberezhskii, Yu.M. and Golikova, E.V., *Kolloidn. Zh.,* 1974, vol. 36.

26. Molodkina, L.M., Golikova, E.V., Bareeva, R.S., Chusov, A.N., and Bogdanova, N.F., *Colloid J.,* 2016, vol. 78, p. 623.
27. Stevens, R., *Zirconia and Zirconia Ceramics,* Magnesium Elektron Ltd. Publ., 1986, no. 113.
28. Jia, Y., Duran, C., Hotta, Y., Sato, K., and Watari, K., *J. Colloid Interface Sci.,* 2005, vol. 291, p. 292.
29. Danelska, A., Ulkowska, U., Socha, R.P., and Szafran, M., *J. Eur. Ceram. Soc.,* 2013, vol. 33, p. 1875.
30. Bowen, P. and Carry, C., *Powder Technol.,* 2002, vol. 128, p. 248.
31. Duran, C., Jia, Y., Hotta, Y., Sato, K., and Watari, K., *J. Mater. Res.,* 2005, vol. 20, p. 1348.
32. Lyklema, J., *Fundamentals of Interface and Colloid Science,* San Diego: Academic Press, 2001, vol. 2.
33. Wiersema, P.H., Loeb, A.L., and Overbeek, J.Th.G., *J. Colloid Interface Sci.,* 1966, vol. 22, p. 78.
34. Molodkina, L.M., Golikova, E.V., Chernoberezhsky, Yu.M., and Kolikov, V.M., *Colloids Surf. A,* 1995, vol. 98, p. 1.

Translated by A. Kirilin